Freie Universität Berlin

Tests for Jumps in Yield Spreads

Lars Winkelmann
Wenying Yao

School of Business & Economics
Discussion Paper

Economics

2021/15

Tests for Jumps in Yield Spreads

Lars Winkelmann*
Department of Economics, Freie Universität Berlin
and
Wenying Yao†
Department of Economics, Deakin University

November 2, 2021

Abstract

This paper develops high-frequency econometric methods to test for jumps in the *spread* of bond yields. We derive a coherent inference procedure that detects a jump in the yield spread only if at least one of the two underlying bonds displays a jump. We formalize the test as a sequential procedure in the context of an intersection union test in multiple testing and introduce a new bivariate jump test for pre-averaged intra-day returns. In an empirical application involving high-frequency data of U.S. government bonds, we contrast response patterns of term spreads and break-even inflation across monetary policy announcements, inflation, and employment news releases.

Keywords: High-frequency data; sequential testing; news announcements; term spread; break-even inflation.

JEL: C58, C12, E43, E44

*The authors gratefully acknowledge financial support by the Deutsche Forschungsgemeinschaft (DFG) through project funding "The Anchoring of Inflation Expectations".

†Corresponding author: Department of Economics, Deakin Business School, Deakin University, 221 Burwood Hwy, Burwood VIC 3125, Australia; Email: wenying.yao@deakin.edu.au.

1 Introduction

News announcement generate significant discontinuities (jumps) in financial asset prices and reveal important information about market expectations and risks. The prevailing presence and high information content of jumps have been demonstrated by the rich literature on jumps as responses to corporate news (Lee and Mykland, 2008; Lee , 2012), macroeconomic news (Lahaye et al., 2011; Jiang et al., 2011), fiscal and monetary policies (Pástor and Veronesi, 2012; Winkelmann et al., 2016). However, the interplay in the response patterns of a pair of bond yields and the spread between them at high-frequency is less known. Yield spreads have long been used to aid financial risk management and policy evaluations. For example, a negative term spread predicts recessions (Henry and Phillips, 2020; Yang, 2020), rising credit spreads inform about increasing default risk (Del Negro and Schorfheide, 2013; Leombroni et al., 2021), and the yield spread between nominal and inflation-indexed government bonds, commonly known as break-even inflation, is a market-based measure of inflation expectations (Chernov and Mueller, 2012; Hanson and Stein, 2015).

This paper develops high-frequency econometric methods to infer a jump in the yield spread of two bonds at a pre-specified point in time.[1] Within the general class of continuous-time semimartingales with Brownian and jump components, the yield spread jumps only if at least one of the underlying bond yield processes jump contemporaneously. However, such coherent test results are not always guaranteed in practice if we only use univariate jump tests, such as the ones proposed by Lee and Mykland (2008) or Lee and Mykland (2012). For instance, a univariate test may detect a jump when it is applied to the yield spread, while it is possible that the same test detects no jump when applied to the two individual bond yields. Figure 1 illustrates the area of incoherent test outcomes in the space of standardized event returns of the two underlying bonds. The dotted area refers to

[1]This point in time can be given by the time of some pre-scheduled news announcement or jump detection method as proposed by Bibinger et al. (2019). Notice that detecting a jump in bond yields opposed to bond prices refers to the same statistical problem.

Figure 1: Confidence sets of the univariate jump test of
Lee and Mykland (2012) in the event return space of bonds a and b.

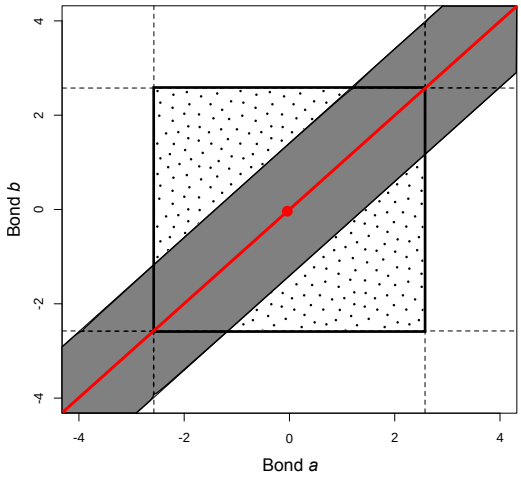

The red dot represents the null hypothesis of no jump in both bond yields, and the red 45° line represents the null of equal yield changes. The dashed lines denote the 0.5% critical values of the univariate Lee and Mykland (2012) jump test applied to the two bonds individually, and the solid square in the middle of the plot outlines the confidence set of no jump in the two bond yields with a family-wise error rate of 1%. The gray shaded area forms the 99% confidence set for the null that the yield changes of the two bonds have the same magnitude using the Lee and Mykland (2012) test on the spread. The dotted area is where incoherent test outcomes occur, i.e., a jump in the yield spread is detected but there is no jump in the two bond yields. The two bond returns are standardized to have unit variance and a correlation of 0.85.

return combinations with contradicting test results, where neither of the two bond yields are tested to contain a jump, but the spread between them displays evidence of a jump. The larger the correlation between the two bonds, the larger the dotted area. To avoid such incoherent results, joint methods for detecting jumps in bond yields and their spread are required.

We propose an intersection union test (IUT) that is based on two nested elementary hypotheses: the hypothesis of no jump in both bond yields (the red dot in Figure 1) and the hypothesis of equal yield changes in the two bonds (the red diagonal line in Figure 1). The first step is to test for a jump in at least one of the two underlying bond yields. If the first step is rejected, we proceed with the second step to test the equality of the two yield changes. The rejection of both elementary hypotheses detects a jump in the spread. The proposed IUT is a special case of step-wise tests that are nested in sequence, and hence

controls the joint error rate without multiplicity adjustment, see Hsu and Berger (1999) and further generalizations by Goeman and Solari (2010). We also show that the IUT procedure fulfills the closure principle of Marcus et al. (1976), which guarantees coherent test results.

Univariate tests for the presence of jumps in discretely observed semimartingale models have been proposed by Aït-Sahalia and Jacod (2009) and Lee and Mykland (2008), for example. Dumitru and Urga (2012) provide an overview and empirical comparison of existing tests. Hansen and Lunde (2006) highlight that trading frictions, such as price discreteness and bid-ask bounces, play a non-trivial role at high observation frequencies. Commonly referred to as the market microstructure noise, these frictions keep observed prices and yields away from discretely observed semimartingales, and distort simple estimators of volatility and jumps. Therefore, Podolski and Ziggel (2010), Aït-Sahalia et al. (2012), Lee and Mykland (2012) and Bibinger et al. (2019) provide noise-robust, univariate jump tests in latent observation models. An extension of the univariate methods to contemporaneous jumps (cojumps) in bivariate semimartingale models is proposed by Jacod and Todorov (2009) and Bibinger and Winkelmann (2015).

Testing for jumps in at least one of the two bond yields in the first step can be accomplished in two different ways. The first approach is to use univariate jump tests on each of the two bond yields with a Bonferroni correction. The Bonferroni approach is conservative in detecting a jump, and can be improved especially when the joint distribution of changes in bond yields under the null is available. We propose a *bivariate jump test* as a more powerful alternative. In a semimartingale model with discrete observations that are corrupted by market microstructure noise, we generalize the univariate pre-averaging methods of Lee and Mykland (2012) and Bibinger and Winkelmann (2015) to the bivariate case. A feasible central limit theorem for a pair of bond returns at some given event time τ under the hypothesis of no jumps, forms the basis of the bivariate jump test. The bivariate

jump test is conceptually different to a cojump test since it has power against jumps in only one of the two bonds. Although the area of incoherent test results does not disappear when combining confidence sets of the bivariate jump test and the univariate test for jumps in the spread, it substantially reduces the area where such conflicting test outcomes can occur.

The limiting distribution of the changes in both bond yields is also used in constructing the test for the equality of event returns in the second step. Since the spread is a simple linear combination of the two underlying bond yields, the test for equal event returns is equivalent to the univariate jump test of Lee and Mykland (2012) applied to the spread. The IUT procedure makes use of the information on jumps in the two underlyinig bond yields when testing jumps in the spread. To put it simply, if the changes in the bond yields are small, the IUT requires a larger movement in the yield spread to detect a jump. In contrast, a single-step univariate jump test on the spread ignores the magnitude of the two bond yield changes. It treats all bond yield changes that result in the same change in the yield spread equally.

The finite sample performance of the two-step IUT procedure is examined using Monte Carlo simulations. We quantify its rate of detecting jumps under different scenarios, and compare the difference in using the Bonferroni and bivariate jump test in the first step of the procedure. Simulation results show that correct classification of jumps depends on the magnitude of the noise variance, sampling frequency, and the size of the jumps in the two bond yields as well as the yield spread. When the noise variance is high, the test procedure has difficulty detecting jumps that are smaller in size. For a given jump size, we can increase the power of the procedure by increasing the frequency of observations over a fixed time interval. Uniformly, across all combinations of jump sizes in bond yields, the IUT based on the bivariate jump test is more powerful in detecting jumps in the spread than the procedure based on the Bonferroni test.

Changes in high-frequency bond yields in response to macroeconomic news releases have become an important tool in empirical macroeconomics and financial economics, see Swanson (2021) and Hanson and Stein (2015) for example. The jump behavior of individual U.S. government bonds and related characteristics have been studied by Jiang et al. (2011) and Hördahl et al. (2020) and the references therein. We demonstrate the IUT procedure using high-frequency data on U.S. government bond yields around prescheduled FOMC announcements, inflation and employment news releases between 2015 and 2020. The jump characteristics of term spreads and break-even inflation rates at different horizons are examined. In contrast to previous papers, we focus on the high-frequency responses of the yield spreads.

The empirical results show that in contrast to jumps in bond yields, jumps in yield spreads are rare. In line with evidence provided by Jiang et al. (2011), we find that bond yields are very sensitive to news releases. The bivariate jump test detects a jump in the underlying bond yields for the majority of all news releases. However, in most cases, these jumps are not accompanied by a jump in yield spreads. Short-horizon yield spreads jump in only 10–20% of the cases where the underlying bond yields display a significant jump. This fraction is almost twice as large for long-horizon yield spreads. While it is well known that employment news releases play an important role in government bond markets, we document that this translates to the movements in yield spreads. The publication of non-farm payroll figures leads to the most frequent and largest jumps in yield spreads. Although responses of yield spreads to monetary policy, inflation and employment news releases differ in the frequency and size of jumps, we find a strong resemblance across the different types of news releases. That is, event returns of bonds that relate to jumps in term spreads or break-event inflation are clustered in very similar regions of the event return space. This suggests a common pattern of comovements in government bonds across the different news releases when they trigger a jump in respective yield spreads. As in the jump regression

model of Li et al. (2017), this insight supports the idea of an underlying factor structure with pairwise constant factor loadings across different event types.

The remainder of the paper is structured as follows. Section 2 introduces the econometric model for the bond yields and the IUT procedure for a jump in the yield spread. Section 3 studies the finite sample properties of the two-step IUT procedure via simulations. After discussing the empirical study in Section 4, we conclude in Section 5. Detailed technical assumptions can be found in Appendix A and proofs in Appendix B. Appendix C contains the list of government bonds used in the empirical section.

2 Econometric method

This section introduces the theoretical framework to investigate jumps in two bond yields and their spread at some fixed point in time using intra-day data observed with market microstructure noise.

2.1 Underlying stochastic process

Let y_t denote the time-t vector of bond yields that relate to the efficient prices of some bond a and bond b.[2] We consider y_t on a normalized interval with some fixed start and end time, surrounding a fixed and known event time τ. The bond yields can be described by a continuous-time bivariate Itô semimartingale:

$$y_t = y_0 + \int_0^t b_s ds + \int_0^t \sigma_s dW_s + J_t, \quad t \in [0, 1]. \tag{1}$$

The continuous part consists of the starting value y_0, a two-dimensional drift b_t, the 2×2 spot-covolatility $\Sigma_t = \sigma_t \sigma_t'$, and a two-dimensional standard Brownian motion W_t.

[2]For a zero coupon bond the relationship between yields, y_t, and prices, P_t, is $y_t^{(i)} = -\log P_t^{(i)}/m^{(i)}$, with time to maturity $m^{(i)}$, $i = a, b$. Detecting jumps in the bond yields and bond prices are interchangeable. Given the focus of the paper, we refer to yields directly instead of log prices.

J_t is a purely discontinuous process that can be completely characterized by its jumps. Assumptions on the different components of y_t are further formalized in Appendix A. Model (1) is fairly general and includes most models for asset prices in financial econometrics, particularly those introduced by Duffie and Kan (1996) for bond yield processes. The occurrence of jumps is not restricted to the event time τ, but can be distributed anywhere on $[0, 1]$. The statistical methods below remain valid, provided that the estimation of covolatility Σ_t is robust to such jumps at $t \neq \tau$.

If we were able to observe the y_t in continuous time, we could have observed all jumps directly. The return $\Delta y_t = y_t - y_{t-}$, $y_{t-} = \lim_{s<t, s\to t} y_s$ is zero in the case of no jump at time t, and $\Delta y_t = \Delta J_t$ otherwise. However, in any practical applications we have only finitely many observations of the two bond yields. We consider observation times t_i, $i = 1, ..., n$, that are discrete, synchronous, and equally spaced across bonds. The sampling interval $t_i - t_{i-1}$ has length $1/n$. Besides the finite n, we follow most of the market microstructure literature and posit an additive, latent observation model in discrete time:

$$\tilde{y}_i = y_{t_i} + \epsilon_i. \tag{2}$$

We observe a noisy version of the efficient process y_{t_i}, where $\epsilon_i \overset{\text{i.i.d}}{\sim} (0, \eta)$, $i = 1, ..., n$, is the market microstructure noise with a 2×2-dimensional covariance matrix η. Aït-Sahalia and Yu (2009) find a negative relationship between the level of the noise variance and different liquidity measures. Less liquid assets usually have larger noise variance. Distorting effects through potential differences in the liquidity of bonds are captured by the noisy observation model (2). Methods to test for significant noise are proposed by Aït-Sahalia and Xiu (2019), for example. Similar to the jump component, increments of the noise term do not vanish asymptotically. Hence, covolatility estimators that are not robust to market microstructure are asymptotically dominated by the noise. Jump detection is

more complicated in cases where jump returns are weakened by the noise while no-jump returns are amplified. Lee and Mykland (2012) highlight the importance of noise-robust jump tests compared to methods that do not account for market microstructure noise. In our setup, market microstructure is an *i.i.d.* process independent of y_t. We extend the model to more general setups in the simulation with endogenous and heteroskedastic noise. Nonsynchronicity of the multivariate data is of less importance, because we focus on a fixed event time τ.

2.2 Bivariate distribution of pre-averaged event returns

Given the noisy observation model (2), smoothing the observed yields is the most intuitive approach to diminish the impact of market microstructure noise. Following the general pre-averaging approaches of Podolskij and Vetter (2009), Jacod et al. (2009) and Christensen et al. (2010), we use the mean of the observed yield vector over M_n discrete noisy observations $\tilde{y}_i = (\tilde{y}_i^{(a)} \;\; \tilde{y}_i^{(b)})'$,

$$\hat{y}_i = M_n^{-1} \sum_{j=i}^{(i+M_n-1)\wedge n} \tilde{y}_j, \quad i = 1, ..., n, \tag{3}$$

where the block length is $M_n = c\sqrt{n}$, and c is a constant tuning parameter. The block length $M_n = c\sqrt{n}$ balances the order of the noise and continuous component of the efficient yields. Since the microstructure noise is centered and serially uncorrelated, taking averages of noisy observations reduces the impact of the noise component. As a result, the estimated return vector at announcement time τ,

$$\Delta\hat{y}_{\tau n} = \hat{y}_{\tau n} - \hat{y}_{\tau n - M_n}, \tag{4}$$

is close to the latent increment of the yield Δy_τ, and is no longer dominated by the noise. The following proposition describes the limiting distribution of the estimated event return

of the two bonds $\Delta\hat{y}_{\tau n} = (\Delta\hat{y}_{\tau n}^{(a)} \;\; \Delta\hat{y}_{\tau n}^{(b)})'$. It is a direct extension of Lemma 1 of Lee and Mykland (2012) and Proposition 3.1 of Bibinger et al. (2019) from the univariate to the bivariate case.

Proposition 2.1 *In the model presented in Section 2.1 under Assumptions 1 and 2 in Appendix A, the return vector* (4) *of pre-averaged yields satisfies*

$$n^{1/4}\left(\Delta\hat{y}_{\tau n} - \Delta y_\tau\right) \xrightarrow{(st)} MN\big(0, \Gamma_\tau\big), \tag{5}$$

where MN denotes a mixed normal distribution, and the 2×2 *covariance matrix* Γ_τ *has elements*

$$\Gamma_\tau^{(i,j)} = 1/3\left(\Sigma_\tau^{(i,j)} + \Sigma_{\tau-}^{(i,j)}\right)c + 2c^{-1}\eta^{(i,j)}, \quad i,j = a,b. \tag{6}$$

Proposition 2.1 shows that the simple pre-averaging approach consistently estimates the event return. The limiting spot variances $\Sigma_\tau^{(i,i)}$, $i = a, b$ and covariance $\Sigma_\tau^{(a,b)}$ can be random (in the case of stochastic volatility, for example), and therefore the limiting distribution in (5) is a mixed normal. The return estimator has the optimal rate of $n^{1/4}$, which is a direct consequence of the choice of the block length M_n and the order of the continuous components of the yield y_t. However, the simple averaging in (3) does not provide an efficient estimator. Bibinger et al. (2019) propose an efficient estimator of jumps in a univariate setting based on spectral statistics. As the variance-covariance matrix in (6) indicates, the diagonal and off-diagonal elements of Γ_τ have the same structure, provided that the microstructure noise displays a covariation $\eta^{(a,b)} \neq 0$ across the bonds a and b. Γ_τ accounts for contemporaneous jumps in (co)volatility by referring to spot (co)volatility before ($\Sigma_{\tau-}$) and at (Σ_τ) the event (see, for example, Bibinger and Winkelmann, 2018; Li et al., 2021, for studies on jumps in (co)volatility).

Stable convergence in law (st) and a consistent estimator of the covariance $\hat{\Gamma}_\tau$ provide a feasible, self-normalizing version of (5), which we will exploit below. Compatible estimators

for integrated (co)volatility and noise in the present modeling context are proposed by Christensen et al. (2010) and Koike (2016).

2.3 A two-step test for jumps in the yield spread

We investigate the joint jump behavior of the two bond yields $y_t^{(a)}$ and $y_t^{(b)}$ and their spread, $y_t^{(a)} - y_t^{(b)}$, at the event time $t = \tau$. Consider the following elementary hypotheses:

- $\mathbb{H}_0^{\mathrm{C}}(\tau)$: $\Delta y_\tau = 0$. The null hypothesis is that there is no jump in both bond yields at time τ, while the alternative, $\mathbb{H}_1^{\mathrm{C}}(\tau)$, allows for jumps in the yields of either bond a or bond b, or both. Section 2.4 introduces a bivariate jump test for this purpose.

- $\mathbb{H}_0^{\mathrm{E}}(\tau)$: $\Delta y_\tau^{(a)} = \Delta y_\tau^{(b)}$. The null hypothesis is that the event returns of bond a and bond b are the same. In other words, the return of the yield spread is zero at time τ. The event returns of the two bonds have different magnitudes under the alternative hypothesis $\mathbb{H}_1^{\mathrm{E}}(\tau)$. Section 2.4 provides a test for this purpose.

Combinations of the two local hypotheses partition the entire event return space into disjoint subsets. We are particularly interested in the following partition:

(A) $= \{\Delta y_\tau : \mathbb{H}_0^{\mathrm{E}}(\tau) \cup \mathbb{H}_0^{\mathrm{C}}(\tau)\}$: Both bond yields do not jump or display a cojump with equal jump size.

(B) $= \{\Delta y_\tau : \mathbb{H}_1^{\mathrm{E}}(\tau) \cap \mathbb{H}_1^{\mathrm{C}}(\tau)\}$: the yield spread jumps.

The classical procedure for the testing problem above is the intersection union test (IUT), which requires both elementary hypotheses to be rejected in order to reject the union (A) (Berger, 1982). Notice that $\mathbb{H}_0^{\mathrm{C}}(\tau)$ is a special case of $\mathbb{H}_0^{\mathrm{E}}(\tau)$. In analog to the step-wise procedure of Hsu and Berger (1999), we first verify the more restrictive hypothesis $\mathbb{H}_0^{\mathrm{C}}(\tau)$ at some level α in the first step, and if $\mathbb{H}_0^{\mathrm{C}}(\tau)$ is rejected, we test $\mathbb{H}_0^{\mathrm{E}}(\tau)$ at level α in the second step. Set (A) is rejected if and only if the hypotheses in both steps are

rejected, in which case the vector of event returns is assigned to set (B). The two-step procedure controls the probability of rejecting at least one true null hypothesis (family-wise error) for all possible configurations of true null hypotheses to be α at most without the need of any multiplicity correction across the two steps. This is in analogue to the closed testing principle of Marcus et al. (1976) to test hypotheses that are nested in sequence, starting with the most restrictive one. In the current context, the closed testing principle requires rejecting the intersection of the two elementary hypotheses $\mathbb{H}_0^{\mathrm{E}}(\tau) \cap \mathbb{H}_0^{\mathrm{C}}(\tau)$ at level α in the first step, before testing $\mathbb{H}_0^{\mathrm{E}}(\tau)$ at level α in the second step. If the hypotheses in both steps are rejected, a jump in the spread is detected. The two steps of the closed test procedure are compatible to those of the IUT procedure. Because $\mathbb{H}_0^{\mathrm{C}}(\tau)$ is a special case of $\mathbb{H}_0^{\mathrm{E}}(\tau)$, testing $\mathbb{H}_0^{\mathrm{E}}(\tau) \cap \mathbb{H}_0^{\mathrm{C}}(\tau)$ is in fact identical to testing the more restrictive hypothesis $\mathbb{H}_0^{\mathrm{C}}(\tau)$. The closed test principle also provides a link to the power considerations in Finner and Strassburger (2002), see also Goeman and Solari (2010). In what follows we propose methods to test $\mathbb{H}_0^{\mathrm{C}}(\tau)$ and $\mathbb{H}_0^{\mathrm{E}}(\tau)$ before investigating the finite-sample performance of the IUT procedure in Section 3.

2.4 χ^2-jump tests

The first step of the IUT procedure requires testing the null hypothesis of no jump in both bond yields at event time τ, $\mathbb{H}_0^{\mathrm{C}}(\tau) : \Delta y_\tau = 0$, against the alternative of a jump in at least one of the two bond yields, $\mathbb{H}_1^{\mathrm{C}}(\tau) : \Delta y_\tau \neq 0$. The most intuitive approach is to consider $\mathbb{H}_0^{\mathrm{C}}(\tau)$ as an intersection hypothesis of two univariate jump tests on the event returns of bonds a and b. This can be achieved using the univariate Lee and Mykland (2012) test,

$$n^{1/4} \, \frac{\Delta \hat{y}_{\tau n}^{(i)}}{\hat{\Gamma}_\tau^{(i,i)}} \xrightarrow{(d)} N(0,1), \quad i = a, b \,, \tag{7}$$

on the event returns of bonds a and b separately with a Bonferroni adjustment. This approach rejects $\mathbb{H}_0^{\mathrm{C}}(\tau)$ as soon as one of the two tests rejects its null hypothesis of no jump at level $\alpha/2$. Such a Bonferroni approach assumes independent test statistics, and thus considers the worst case scenario. It is the most conservative in testing $\mathbb{H}_0^{\mathrm{C}}(\tau)$ and consequently in testing the union hypothesis $\mathbb{H}_0^{\mathrm{E}}(\tau) \cup \mathbb{H}_0^{\mathrm{C}}(\tau)$ of the IUT. We can improve on the Bonferroni test using the χ^2-*jump test* stated in Corollary 2.2.

Corollary 2.2 *Given Proposition 2.1, the bivariate χ^2-jump test at the event time τ refers to the following test statistic and asymptotic distribution under $\mathbb{H}_0^{\mathrm{C}}(\tau)$:*

$$\sqrt{n}\ \Delta\hat{y}'_{\tau n}\hat{\Gamma}_\tau^{-1}\Delta\hat{y}_{\tau n} \xrightarrow{(d)} \chi^2(2). \tag{8}$$

The χ^2-jump test has critical region

$$\left\{\sqrt{n}\ \Delta\hat{y}'_{\tau n}\hat{\Gamma}_\tau^{-1}\Delta\hat{y}_{\tau n} > q_{1-\alpha}(\chi^2(2))\right\}, \tag{9}$$

where $q_{1-\alpha}(\chi^2(2))$ denotes an upper quantile of the χ^2 distribution with two degrees of freedom at significance level α. The bivariate test has asymptotic level α under $\mathbb{H}_0^{\mathrm{C}}(\tau)$. The test is consistent under the alternative $\mathbb{H}_1^{\mathrm{C}}(\tau)$ with divergence rate $n^{1/2}$.

Corollary 2.2 shows a standard result in multivariate statistics for the sum of squares of the vector of whitened event returns, $z_\tau = \hat{\Gamma}_\tau^{-1/2}\Delta\hat{y}_{\tau n}$. Under $\mathbb{H}_0^{\mathrm{C}}(\tau)$, elements of the 2×1 vector $n^{1/4}z_\tau$ are independent standard normal random variables. As a result, the sum of squares $\sqrt{n}\, z_\tau\prime z_\tau$ in (8) has an asymptotic χ^2 distribution with two degrees of freedom. The $\sqrt{n}$ convergence rate is a direct consequence of the $n^{1/4}$ rate of pre-averaged returns in Proposition 2.1.

Corollary 2.2 also provides a method to test the magnitude of the two returns in the second step. The aim is to distinguish the null hypothesis of equal yield changes of bonds

a and b, $\mathbb{H}_0^{\mathrm{E}}(\tau) : \Delta y_\tau^{(a)} = \Delta y_\tau^{(b)}$, against the alternative of different return sizes, $\mathbb{H}_1^{\mathrm{E}}(\tau) : \Delta y_\tau^{(a)} \neq \Delta y_\tau^{(b)}$. We impose a linear restriction, $R' = (1 \ \ -1)$, on the χ^2-test statistic in Corollary 2.2, which transforms (8) under $\mathbb{H}_0^{\mathrm{E}}(\tau)$ into

$$\sqrt{n}\,(R'\Delta\hat{y}_{\tau n})(R'\hat{\Gamma}_\tau R)^{-1}(R'\Delta\hat{y}_{\tau n}) \xrightarrow{(d)} \chi^2(1). \tag{10}$$

The test statistic (10) takes the square of the estimated event returns of bond a and bond b, $\left(n^{1/4}(\Delta\hat{y}_{\tau n}^{(a)} - \Delta\hat{y}_{\tau n}^{(b)})\right)^2$, and divides it by the variance of the difference $R'\hat{\Gamma}_\tau R$. This test statistic is equivalent to the square of the univariate statistic of Lee and Mykland (2012) in (7), applied to the yield spread. Hence, testing for equal event returns is equivalent to a univariate test for no jump in the spread.

Figure 2 combines the two elementary jump tests to illustrate the partitions (A) and (B) of the two-step IUT procedure on the two-dimensional space of event returns of bond a and bond b. The test procedure uses a significance level of 1%, and the two bond returns are standardized to have unit variance and a correlation of $\rho = 0.85$. The left panel uses the Bonferroni-adjusted univariate Lee and Mykland (2012) test on the two bond yields in the first step, which gives the square shaped confidence set. Its union with the 45° corridor, which is the confidence set for the univariate jump test on the spread in the second step, forms the area of set (A). The right panel uses the χ^2 bivaraite jump test in the first step, which leads to a much smaller confidence set compared with the Bonferroni-adjusted approach shown in the left panel. It is worth noting that the elliptical shape of the χ^2 confidence set and the width of the diagonal corridors are influenced by the correlation ρ between the two bonds. Considering the whitened and standardized case with $z_\tau = \hat{\Gamma}_\tau^{-1/2}\Delta\hat{y}_{\tau n}$, the χ^2 confidence set is a circle and the diagonal corridor widens. Given the empirical observation that bond yields are usually positively correlated, varying degree of elliptical shape is common in practice. Its union with the 45° corridor defines

Figure 2: Partitions (A) and (B) of the IUT for jumps in yield spreads in the event return space of bonds a and b.

(a) Bonferroni (b) χ^2 bivariate jump test

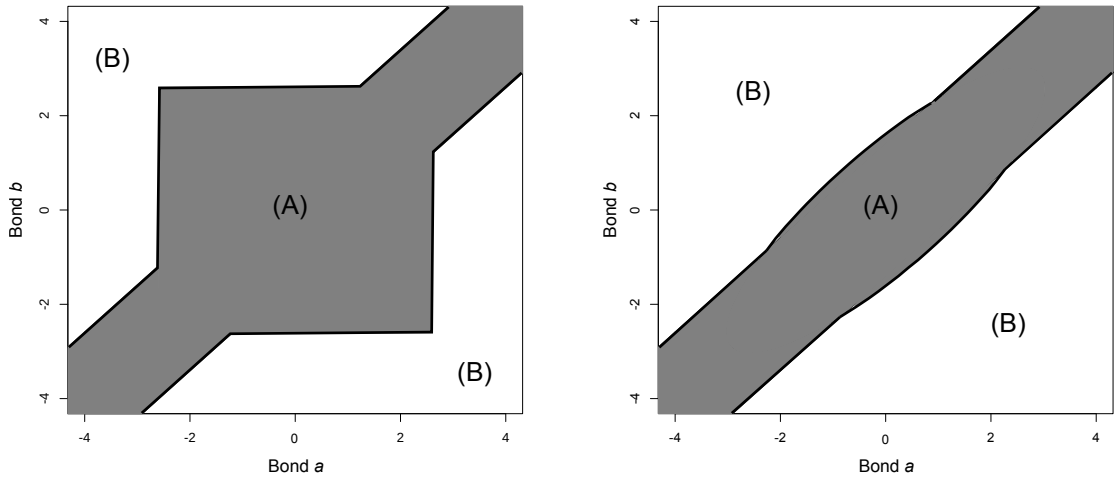

The gray shaded area indicates the region where the union null $(A) = \{\Delta y_\tau : \mathbb{H}_0^{\mathrm{E}}(\tau) \cup \mathbb{H}_0^{\mathrm{C}}(\tau)\}$ of no jump in the spread is not rejected with family-wise error rate of 1%. The two white areas form the intersection alternative $(B) = \{\Delta y_\tau : \mathbb{H}_1^{\mathrm{E}}(\tau) \cap \mathbb{H}_1^{\mathrm{C}}(\tau)\}$, where a jump in the yield spread is detected. The two bond returns are standardized to have unit variance and a correlation of 0.85.

the area of set (A) where a jump in the yield spread is not detected. It is evident that the χ^2-based IUT procedure leads to a smaller area for set (A). Hence, compared with the Bonferroni-adjusted approach, the χ^2-based IUT is more powerful in detecting jumps across all combinations of event returns for bonds a and b. Finally, the cost of the χ^2-based IUT in achieving coherent test outcomes relative to testing only the spread for a jump seems small. The rejection area of the IUT in panel (b) of Figure 2 is close to that of the univariate jump test on the spread. We quantify those differences in finite sample in the simulation study below.

3 Simulation study

We use simulations to examine the finite-sample properties of the two-step IUT procedure. The test for equal event returns is equivalent to the univariate Lee-Mykland jump test,

whose properties has been examined by Lee and Mykland (2012) and Bibinger et al. (2019). Therefore, we do not repeat this exercise here. The simulation setup emulates that of Lee and Mykland (2012) and captures some key characteristics of the empirical data used in Section 4.

We consider observations of the two bond yields on a three-hour time interval that is centered around the event time τ. The yield of bond a is generated by

$$y_t^{(a)} = 1 + \int_0^t \sigma_s \, dW_s + J_t^{(a)}, \quad t \in (0, 1], \tag{11}$$

with a Heston-type stochastic volatility

$$d\sigma_s^2 = 0.0162 \left(0.8465 - \sigma_s^2\right) ds + 0.117 \, \sigma_s \, dB_s, \tag{12}$$

where B_t and W_t are two independent standard Brownian motions. We adopt the parameter values of Lee and Mykland (2012) and assume 252 trading days per year with 9 hours of trading on each day. The yield of bond b is

$$y_t^{(b)} = \rho \left(1 + \int_0^t \sigma_s dW_s\right) + \sqrt{1 - \rho^2} \int_0^t d\tilde{W}_s + J_t^{(b)}, \quad t \in (0, 1], \tag{13}$$

where ρ is the correlation between the continuous components of the two bond yields, and $\tilde{W}_t$ is a standard Brownian motion that is independent of B_t and W_t. The correlation is fixed to be $\rho = 0.85$, which is the average correlation of the 10-year nominal and inflation-indexed bonds in the data studied in Section 4. We set the jump process in both bond yields to be $J_t = 0$ for $t < \tau$ and $J_t = \Delta J_\tau$ for $t \geq \tau$. Three different jump sizes are considered at $t = \tau$: small jump $\Delta J_\tau^{(i)} = 0.3$, medium jump $\Delta J_\tau^{(i)} = 0.6$, and large jump

$\Delta J_\tau^{(i)} = 1$, $i = a, b$. The market microstructure noise is generated by

$$\epsilon_i^{(j)} = 0.0861 \Delta y_{t_i}^{(j)} + 0.06\big(\Delta y_{t_i}^{(j)} + \Delta y_{t_{i-1}}^{(j)}\big) + U_i, \quad i = 0, \ldots, n, \quad j = a, b, \tag{14}$$

where $(U_i)_{0 \le i \le n}$ is a sequence of normally distributed random variables with mean 0 and variance q^2. We consider two parameterizations of q, 0.1 and 0.01, which governs the noise level (market quality parameter). The cross-correlation between the yields y_t and the noise violates one of our theoretical assumptions. However, simulation results show that this correlation does not affect the finite-sample performance of the test. Therefore, we work with this more general and realistic setting. The (co)volatility and noise are estimated using the approach of Christensen et al. (2010). The pre-averaging estimator of (co)volatility uses a window size of $\sqrt{n}/3$, while the jump tests use a block size of $M_n = \sqrt{n}/18$. The constant $c = 1/18$ is chosen according to Table 5 of Lee and Mykland (2012).

Table 1 shows the rejection frequencies of set (A) using the two-step IUT proecedure at level $\alpha = 1\%$. The first column reports two different sampling frequencies of 30-second and 5-second, with their respective sample sizes in parentheses. Two different procedures are recorded in the second column of Table 1. The first approach uses two univariate jump tests with a Bonferroni adjustment in its first step, while the second approach uses the χ^2-jump test from Corollary 2.2 in its first step. The second step of the two procedures are identical, which uses the χ^2 test for equal event returns. The jump sizes reported in columns three and four belong to the union null hypothesis of set (A), while all other columns correspond to the intersection alternative (B) of a jump in the spread. Both of the two test procedures exhibit good size properties, with actual sizes below the nominal level of 1% in all cases. In the case of equal jump sizes shown in column four, the first step tests detect the medium sized jumps with high probability, such that the outcome of the IUT is almost fully determined by the test for equal returns in the second step. Differences

Table 1: Rejection frequencies of set (A) using the two-step IUT procedure.

Jump size bond a		0	0.6	0.3	0.6	1	0.6	1
Jump size bond b		0	0.6	0	0	0	0.3	0.3
Noise level: $q = 0.01$								
30-sec (n=360)	Bonferroni	0.005	0.001	0.053	0.556	0.949	0.380	0.935
	χ^2 test	0.005	0.002	0.220	0.994	1.000	0.590	1.000
5-sec (n=2160)	Bonferroni	0.003	0.009	0.470	1.000	1.000	0.994	1.000
	χ^2 test	0.007	0.009	0.945	1.000	1.000	1.000	1.000
Noise level: $q = 0.1$								
30-sec (n=360)	Bonferroni	0.000	0.001	0.011	0.396	0.883	0.111	0.826
	χ^2 test	0.000	0.001	0.031	0.705	0.998	0.148	0.909
5-sec (n=2160)	Bonferroni	0.003	0.007	0.188	0.982	1.000	0.748	1.000
	χ^2 test	0.005	0.007	0.324	1.000	1.000	0.757	1.000

The average volatility for the two bond yields on the three-hour block is $\sqrt{0.8465/(252 \times 3)}$. Tests are conducted at nominal level of $\alpha = 1\%$ using 3,000 repetitions. Rows labeled Bonferroni refer to the two-step IUT procedure where the univariate Lee and Mykland (2012) test is used to test for jumps in the two bond yields at level $\alpha/2 = 0.5\%$ in the first step. Rows labeled χ^2 test implement the $\chi^2(2)$ test (8) in the first step. Jump sizes and noise levels are reported in basis points.

between the Bonferroni and χ^2 procedures and different noise levels are small under the union null hypothesis.

The scenario where only one of the two bond yields contains a jump is studied in columns five to seven of Table 1. The magnitude of the small jump is less than two times the spot volatility in the case of 30-second sampling. Therefore, it is not surprising that both IUT procedures have difficulties in detecting the jump in the spread. Under the 30-second sampling scheme, both the Bonferroni and χ^2 test detect no jump in the spread with high probabilities. This problem is aggravated by higher noise levels. However, once the size of the spread jump increases, or the observation frequency increases to 5-second, the percentage of correctly detecting a jump in the spread quickly approaches 100%. The Bonferroni approach almost always has lower power than the χ^2 approach, because it does not make use of the information about the correlation of the two bond yields. The power

gain in using the χ^2 approach is particularly large in the case of medium sized jump, high noise level, and low sampling frequency.

Columns eight and nine of Table 1 report the results for the cases where both asset prices cojump but with different magnitudes. The difference between the Bonferroni and χ^2 test becomes small. This is because the medium and large sized jumps in bond a are easily detected in the first step by either of the two approaches, and the test for equal event returns in the second step is identical. Comparing column eight and column five, both of which have a spread jump of size 0.3, the detection rate is higher when both bond yields have jumps than when only one bond yield has a jump. The improvement in detecting spread jumps is more pronounced for the Bonferroni approach and when the sampling frequency is high.

In summary, the IUT procedure has good size under the union null hypothesis of no jump in the spread, but its power depends on a few factors. Firstly, larger jump size in the spread leads to higher power, which is expected. Secondly, a higher noise level reduces the power, especially when the observation frequency is low and the jump size is small. When the observation frequency is high and the jump in the spread has medium or large size, the noise level only has very limited impact on the performance of the testing procedure. Thirdly, the IUT based on the χ^2-jump test dominates the Bonferroni-based approach uniformly, which is shown in Figure 2, and we also demonstrate in finite sample in Figure 3.

Panel (a) of Figure 3 illustrates the power gain of the IUT based on the χ^2 test over the Bonferroni-based IUT test. Across all combinations of event returns for bond a bond b, the χ^2 procedure has at least the same power as the Bonferroni approach. If the jumps in the two bond yields fall in the colored areas, the χ^2-based IUT procedure has a higher probability of correctly identifying a jump in the spread than the Bonferroni-based IUT procedure. The power gain can reach up to 80% in the darker shaded areas. The region

Figure 3: Power gaps.

(a) Power gain IUT: χ^2 vs. Bonferroni

(b) Power loss: χ^2-based IUT v.s. univariate jump test on the spread

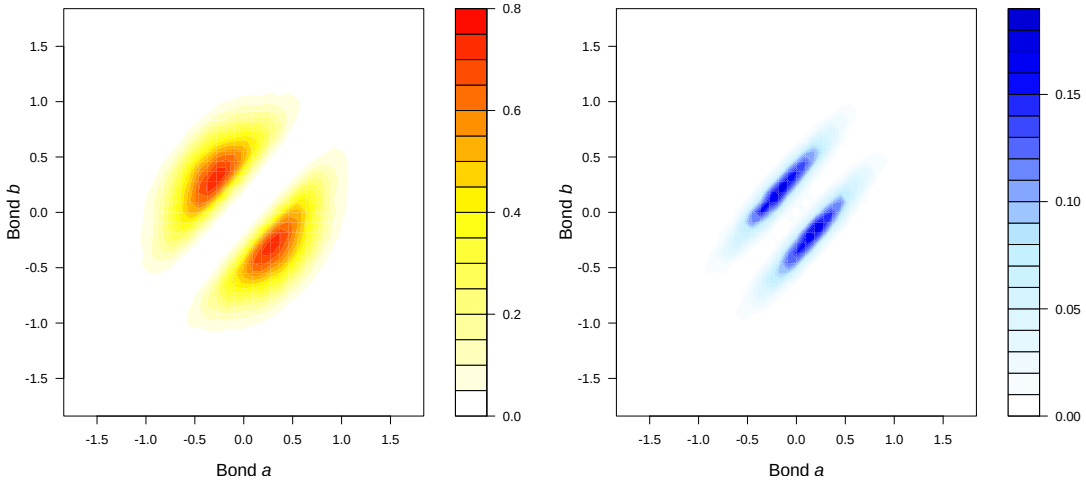

For any combination of yield changes of bond a (x-axis) and b (y-axis), Panel (a) shows the power gain of the IUT procedure based on the bivariate χ^2-jump test over the Bonferroni-based IUT approach. Panel (b) shows the power loss of the IUT based on the bivariate jump test over the univariate jump test on the spread. Darker red (blue) color signals higher power gain (loss). Data are simulated with $n = 360$, $q = 0.01$. Other parameters are chosen as described above.

where the χ^2 test exhibits power gains has a similar shape to the region of incoherent test results depicted in Figure 1 (the dotted area).

Panel (b) of Figure 3 depicts the power loss of using the two-step IUT procedure based on the χ^2 test compared with the univariate jump test on the spread alone. This can be interpreted as the cost to pay in order to achieve a coherent test for jumps in the spread. The loss in power is driven by the fact that part of the confidence region of the χ^2 bivariate jump test is outside the confidence region of the univariate jump test on the spread. These areas will always exist, because the confidence set of the χ^2 test can never be a subset of the confidence set of the univariate jump test on the spread when both of them are conducted at the same significance level. The colored areas show the jump sizes in the two bond yields where the univariate jump test on the spread has higher probability of correctly identifying a jump in the spread than the IUT procedure based on the χ^2 bivariate jump test. In

our simulation, the areas of power loss in the event-return space appear non-negligible, the power loss never exceeds 20%. Instead of assuming that jump sizes are known and interpreting the blue colored area as a loss, in practice jump sizes need to be estimated and estimated jump sizes in the blue colored region are likely to belong to the null hypothesis of no jumps in bond yields and therefore should be taken as evidence against a jump in the yield spread.

4 Empirical evidence

We use the two-step IUT procedure to test for jumps in the term spread and break-even inflation at major news announcement times in the U.S.. We focus on the χ^2-based approach given its superior properties demonstrated above.

4.1 Yield spread data

We study 41 pre-scheduled federal open market committee (FOMC) announcements, 63 consumer price inflation (CPI) and 47 non-farm payroll (NFP) news releases between January 2015 and March 2020. For each release date, we download yield quotes on an interval spanning from one-hour before to one and a half hour after the publication time. The publication times are 2:00 p.m. EST for the FOMC statements and 8:30 a.m. EST for the CPI and NFP releases. Our empirical analyses use 30-seconds mid-quotes of specific U.S. Treasury bonds with maturities close to 2, 10 and 20 years. In addition to the nominal bonds, we also consider inflation-indexed bonds, which compensate investors for inflation and thereby provide measures of real interest rates. The entire list of bonds and their detailed information are given in Appendix C. The data are obtained from Refinitiv DataScope Select provided by Thomson Reuters Tick History.

Table 2 presents the descriptive statistics of the nominal and inflation-indexed bond

Table 2: Descriptive statistics of government bond yields and yield spreads.

Maturity	Nominal bonds			Indexed bonds		Term spread		Break-even inflation	
	2Y	10Y	20Y	2Y	10Y	2Y10Y	2Y20Y	BEI2Y	BEI10Y
Panel A: observed 30-second returns									
ave($\Delta\tilde{y}_i$)	-0.003	-0.005	-0.004	-0.007	-0.006	-0.002	-0.001	0.004	0.000
std($\Delta\tilde{y}_i$)	0.483	0.259	0.216	0.392	0.276	0.334	0.332	0.410	0.223
med($\lvert\Delta\tilde{y}_i\rvert$)	0.390	0.300	0.200	0.500	0.300	0.300	0.290	0.405	0.020
Panel B: microstructure noise									
p-value	0.000	0.147	0.179	0.000	0.127	0.007	0.057	0.000	0.000
rejection rate	0.709	0.391	0.311	0.695	0.378	0.676	0.483	0.808	0.748
noise level η	0.121	0.121	0.103	0.152	0.124	0.154	0.146	0.176	0.066

The bond data are 30-second observations in the 2.5-hour window around FOMC announcements, CPI and non-farm payroll news releases from January 2015 to March 2020. All statistics are in basis points. The p-value refers to the autocorrelation based test for microstructure noise proposed by Aït-Sahalia and Xiu (2019). The fraction of rejecting the null of no noise using the same test at 5% significance level is reported in row labeled rejection rate. The average noise level is estimated using Proposition 1 of Lee and Mykland (2012).

yields, as well as the respective spreads. We study two term spreads and two break-even inflation rates at different horizons: the yield differential between the 10-year and 2-year nominal bonds (2Y10Y), the 20-year and 2-year nominal bonds (2Y20Y), the 2-year nominal and inflation-indexed bonds (BEI2Y), and the 10-year nominal and inflation-indexed bonds. Panel A of Table 2 shows the mean and standard deviation of observed 30-second yield changes in basis points. The average yield change is always close to zero, and the standard deviation varies between 0.2 to 0.5 basis points. The last row in Panel A presents the median of the absolute 30-second yield change to gauge the typical movements in each series. All of them are well below one basis point and decrease as the horizon increases. This trend is in line with the smaller standard deviation for longer-horizon series.

Panel B of Table 2 provides evidence on the prevalence of market microstructure noise in the bond data. We report the median p-value and the percentage of rejections at a 5% level for the autocorrelation based noise test proposed by Aït-Sahalia and Xiu (2019). The small p-values and high rejection rates of no noise, particularly for shorter-term bond yields

and yield spreads, support the importance of our noise-robust method proposed in Section 2. The noise level in the last row of Table 2 reports the average value of the estimated η, obtained using the noise estimator of Lee and Mykland (2012). This estimator has the ability to account for autocorrelated noise and jumps in the bond yields. The noise level has similar magnitudes to the high noise level used in the simulation in Section 3 across different bonds and spreads.

We also examine the time-variation of spreads over the 2.5-hour time interval around news announcements. Figure 4 depicts the 10% and 90% quantiles of observed changes in the 20-year-2-year term spread and 10-year break-even inflation across the 41 FOMC announcements. It is evident that the return of the 20-year-2-year term spread has higher variations than that of the 10-year break-even inflation, consistent with the statistics from Table 2. The FOMC press release time at 2:00 p.m. is accompanied by a spike in the quantile range in both panels. The quantile range widens after the announcement time,

Figure 4: Quantile range of changes in yield spreads around FOMC announcements.

(a) 20-year-2-year term spread (b) 10-year break-even inflation

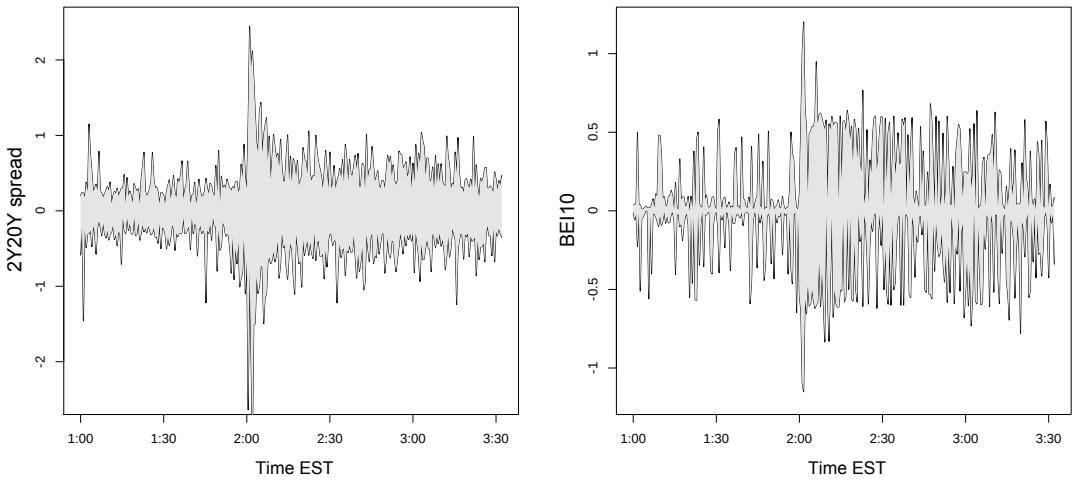

This figure depicts the 10% and 90% quantile of 30-second changes in the spread of bond yields in basis points across 41 FOMC announcements in the sample. Panel (a) depicts the spread between the 20-year and 2-year nominal bond yields, and Panel (b) shows the yield spread between the 10-year nominal and inflation-indexed bonds.

suggesting larger post-event variance in the spread. The post-event volatility is estimated below using data starting from 30 minutes after the announcement time. Figure 4 also suggests the existence of gradual jumps, *i.e.* the yield adjustments pick up slightly before the announcement time in some cases, and trigger strongly elevated returns over a few 30-second observations. Therefore, instead of using Equation (4) to estimate the event return, we use $\Delta\hat{P}_{\tau n} = \hat{P}_{\tau n+2} - \hat{P}_{\tau n-M_n-1}$. That is, the three return observations from 30-second pre-announcement to 1-minute post-announcement are all included in the estimated event return. The gradual adjustment may be considered a feature of the market microstructure noise, which results from a thin order book as discussed at length by Barndorff-Nielsen et al. (2009). Further details on the estimation and the testing procedure are discussed in the next section.

4.2 Jumps in yield spreads

One advantage of high-frequency statistical methods is that we can zoom in on each individual announcement or news release separately, and analyze their distinct effects on the bond yields and yield spreads. We examine locally around each news release whether the yield spreads jump using the two-step IUT procedure based on the χ^2 test and estimate their jump sizes. Parameter values for the pre-average return and volatility estimation are chosen as described in Sections 3 and 4.1. In estimating the pre- and post-event volatility, we use 1-hour estimation windows starting from one hour before and half an hour after the event time, respectively. Furthermore, thresholding techniques are employed to remove jumps that may occur within those estimation windows. In line with the pre-averaging methods proposed by Koike (2016), we apply a universal threshold based on the median absolute deviations of the pre-average returns for volatility estimation. The volatility is estimated using pre-averaged yields of three-minute windows.

Table 3 summarizes the results from the two-step testing procedure. For each event

Table 3: Rejection frequencies in each step of the IUT test procedure at news release times between 2015 and 2020.

		Term spread		Break-even inflation	
Event	Jump	2Y10Y	2Y20Y	BEI2Y	BEI10Y
Monetary policy:	Bond yields (Step 1)	0.659	0.683	0.537	0.268
41 FOMC releases	Yield spread (Step 2)	0.073	0.268	0.073	0.073
Inflation:	Bond yields (Step 1)	0.571	0.571	0.476	0.349
63 CPI releases	Yield spread (Step 2)	0.111	0.159	0.063	0.127
Employment:	Bond yields (Step 1)	0.851	0.872	0.872	0.532
47 NFP releases	Yield spread (Step 2)	0.106	0.340	0.191	0.128

Term spread refers to the spread between a pair of nominal U.S. government bond yields with a 10-year and 2-year maturity (2Y10Y) and a 20-year and 2-year maturity (2Y20Y), respectively. Break-even inflation is the spread between a nominal and an inflation-indexed bond yields of the same maturity. We consider the 2-year (BEI2Y) and 10-year (BEI10Y) break-even inflation. We use the 1% level of significance and a 1.5-minute jump window at the announcement time to allow for delayed or gradual adjustments. The number in the row for the bond yields (Step 1) represents the fraction of the total number of news releases where the bivariate χ^2-jump test rejects the null of no jump in the two asset prices. The number in the row for the yield spread (Step 2) represents conditional on a rejection in the first step, the fraction of news releases where the test for equal event returns is rejected.

type and the four different yield spreads, we report the frequencies of detecting a jump in at least one of the two bond yields (Step 1) and detecting a jump in the spread between them (Step 2). These results show that for all three types of news releases, usually more than 50% of them trigger a jump in at least one of the two bond yields. The largest percentages come from the release of non-farm payrolls, where about 87% of all 47 news releases are associated with a jump in either the 2-year, 10-year or 20-year bond yields. However, this high probability of jumps in the bond yields across the different events does not translate to jumps in the yield spreads. The occurrence of jumps in spreads is much less likely, ranging from 6.3% to 34% of the respective releases. Comparing the percentages of jumps in bond yields and jumps in yield spreads for each event type, it appears that for the shorter-horizon in columns three and five, roughly 10–20% of the jumps in bond yields are accompanied by a jump in yield spreads. A similar homogeneity across the types of

news releases exists for the longer-horizon yield spreads reported in column four and six. However, the fraction of the jumps in bond yields that are accompanied by a jump in yield spreads is around 25–40%.

To obtain a better understanding of the response patterns of the bond yields and spreads across different news releases, Figure 5 shows the scatter plots of the estimated event returns of two pairs of bond yields. We use the 2-year and 20-year bond yields (left column) and 10-year nominal and inflation-indexed bond yields (right column) as examples, but other combinations of bond yields show similar patterns. The empty circles represent the situations where the two-step IUT procedure based on the χ^2 bivariate jump test does not detect a jump in the spread, and the green circles denote the pairs of event returns where a jump is detected in their spread. It is evident from Figure 5 that across all three types of news releases, the term spread and break-even inflation do not jump in most cases. The combinations of event returns that relate to significant jumps in yield spreads are further away from the 45° line for the term spread than for break-even inflation. This implies that the region (A), where no jump in the yield spread can be detected, is usually wider for the term spread than for break-even inflation. As a result, some pairs of event returns that appear quite far away from the 45° line are not classified as jumps in the term spread, while they would suffice to be detected as a jump in break-even inflation.

Despite the varying frequencies and magnitudes of jump sizes, the plots show a high degree of similarity across the monetary policy, inflation and employment news releases. Event returns that are associated with a jump in the respective yield spread seem to cluster around a very similar area across the different types of news announcements. Jumps in the term spread usually result from much stronger yield adjustments in the 2-year bond compared with the 20-year bond. Jumps in the break-even inflation rates are usually associated with stronger responses in the nominal than the inflation-indexed bond yields. This implies that over the time period from 2015 to 2020, the news releases that have

Figure 5: Estimated even returns of U.S. government bonds at news release times in 2015–2020.

(a) Term spread: Monetary policy

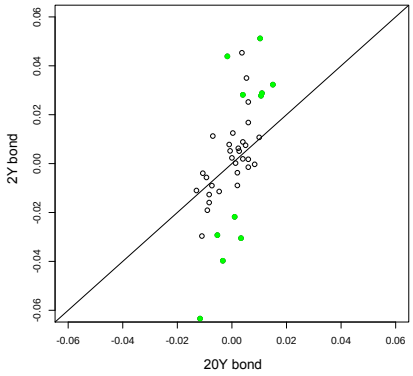

(b) BEI: Monetary policy

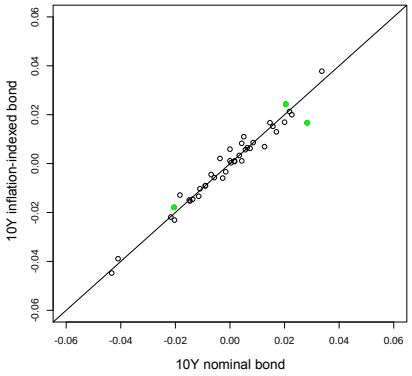

(c) Term spread: Inflation

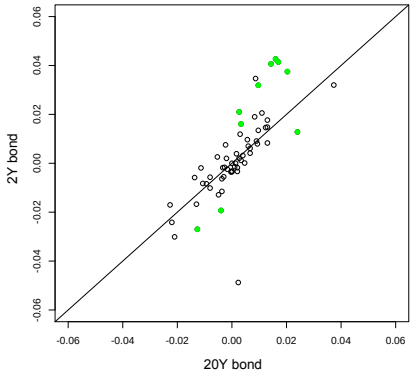

(d) BEI: Inflation

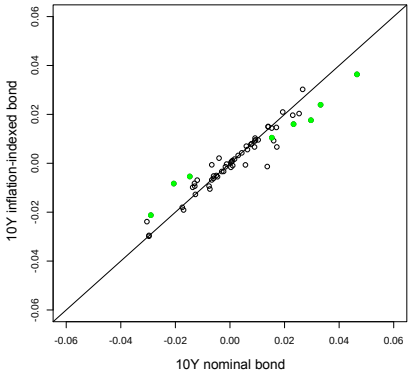

(e) Term spread: Employment

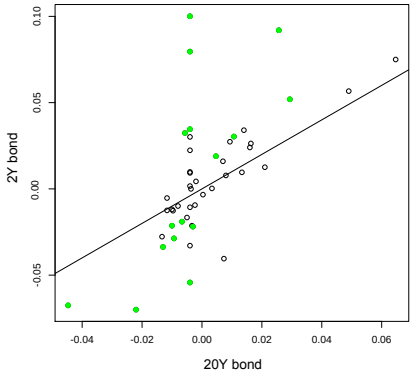

(f) BEI: Employment

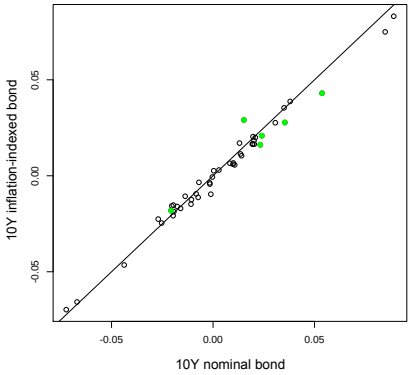

Panels in the left column depict the estimated event returns for nominal bonds with 20 years (20Y) and 2 years (2Y) maturity. Panels in the right column plot the estimated event returns for the 10-year nominal and inflation-indexed bonds. Based on the IUT procedure, the empty circles represent situations without a jump in the respective yield spread. The green circles represent cases where a jump in the spread is detected at the 1% level. The event returns are estimated using a 1.5-minute jump window.

significant effects on yield spreads tend to narrow the term spread and increase the break-even inflation.

Table 4 shows the average magnitude of jumps in the yield spreads for the three different news releases. The release of non-farm payroll data has the strongest impact on the term spreads and break-even inflation. It alters the 10-year-2-year term spread by 4 basis points on average, and the 2-year break-even inflation by 3.2 basis points. In comparison with the median absolute change in the yield spreads across all 30-second observations reported in Table 2, the average size of the spread jump is huge. Consistent with the result from Table 3 where the FOMC announcements lead to the fewest number of jumps in break-even inflation, they also result in the smallest jump sizes of 1.9 and 0.6 basis points. Still, compared with median absolute changes in the yield spreads, these detected jumps are sizeable.

Table 4: Average jump size of yield spreads in basis points at news release times between January 2015 and March 2020.

Event	Term spread		Break-even inflation	
	2Y10Y	2Y20Y	BEI2Y	BEI10Y
Monetary policy	1.903	3.013	1.880	0.606
Inflation	1.430	1.887	2.259	0.913
Employment	4.000	3.693	3.155	0.749

The number in each cell shows the average of absolute jump return in basis points. Jump sizes are estimated using 1.5-minute window at the announcement times.

5 Conclusion

This paper argues that inference about jumps in the yield spread of two bonds requires a joint approach that includes evidence on jumps in the two underlying bond yield processes. This requirement is an immediate consequence of the high-frequency model, where a jump in the spread exists only if at least one of the underlying yield processes has a jump. Ignoring this inherent connection by basing inference only on a univariate jump test applied to the spread tends to overestimate the number of jumps in yield spreads and puts the coherence of test results at risk. We propose an intersection union test (IUT) for jumps in the spread, which explicitly takes into account the joint jump behavior of the two bond yields and their spread. The proposed IUT uses a two-step procedure that includes testing the hypothesis of no jumps in both underlying bond yields against a jump in at least one of the two yield processes. We propose a bivariate jump test for this task. The methods we employ are robust to the presence of market microstructure noise in the observed bond yield data. Monte Carlo simulations reveal good finite sample properties of the proposed two-step test procedure.

We use the two-step IUT procedure to analyze high-frequency responses of government bond yields to monetary policy announcements, inflation and employment releases in the period of 2015–2020. Focusing on two term spreads and two break-even inflation rates at different horizons, the empirical results show that in contrast to jumps in bond yields, jumps in term spreads and break-even inflation are rare events. Despite differences in the frequency and magnitude of jumps in yield spreads across the different types of news releases, our analyses show that the respective high-frequency response pattern of the underlying bond yields are quite similar. Given the distinct information content of monetary policy, inflation and employment news releases, this homogeneity deserves more comprehensive empirical investigations that go beyond the purpose of the present paper.

Although the methodology proposed in this paper is illustrated in the context of government bonds and yield spreads, it can directly be applied to other high-frequency asset price data. For example, stocks that are cross-listed in different stock exchanges are expected to have the same movements under the different listings. We can use the IUT procedure to discover mis-pricing or synergies between them, especially at the time when earnings announcements are released.

References

Aït-Sahalia, Y., and Jacod, J. (2009), *Testing for jumps in a discretely observed process*, Annals of Statistics 37, 184–222.

Aït-Sahalia, Y., and Jacod, J. and Li, J. (2012), *Testing for jumps in noisy high frequency data*. Journal of Econometrics 168, 207–222.

Aït-Sahalia, Y. and Xiu, D. (2019), *A Hausman test for the presence of noise in high frequency data*, Journal of Econometrics 211, 176–205.

Aït-Sahalia, Y. and Yu, J. (2009), *High-frequency market microstructure noise estimates and liquidity measures*, Annals of Applied Statistics 3, 422–457.

Barndorff-Nielsen, O., Hansen, P., Lunde, A. and Shephard, N. (2009), *Realized Kernels in Practice: Trades and Quotes*, Econometrics Journal,12, C1–C32.

Berger, R.L. (1982), *Multi-parameter hypothesis testing and acceptance sampling*, Technometrics 24, , 295?300.

Bibinger, M., Neely, C.J. and Winkelmann, L. (2019).*Estimation of the discontinuous leverage effect: Evidence from the NASDAQ order book*, Journal of Econometrics 209, 158–184.

Bibinger, M. and Winkelmann, L. (2015) *Econometrics of cojumps in high-frequency data with noise*, Journal of Econometrics 184 (2), 361–378.

Bibinger, M. and Winkelmann, L. (2018) *Common price and volatility jumps in noisy high-frequency data*, Electronic Journal of Statistics 12, 2018–2073.

Chernov, M. and Mueller, P. (2012) *The term structure of inflation expectations*, Journal of Financial Economics 106, 367–394

Christensen, K., Kinnebrock, S. and Podolskij, M. (2010), *Pre-averaging estimators of the ex-post covariance matrix in noisy diffusion models with non-synchronous data*, Journal of Econometrics 159, 116–133.

Del Negro, M. and Schorfheide, F. (2013), *DSGE Model-Based Forecasting*, Handbook of Economic Forecasting 2, Elsevier, 57–140.

Duffie, D. and Kan, R. (1996), *A yield-factor model of interest rates*, Mathematical Finance 6, 379–406.

Dumitru, A.M. and Urga, G. (2012) *Identifying Jumps in Financial Assets: A Comparison Between Nonparametric Jump Tests*, Journal of Business and Economic Statistics 30, 242–255.

Finner, H. and Strassburger, K. (2002),*The partitioning principle: A powerful tool in multiple decision theory*, Annals of Statistics, 30, 1194–1213.

Goeman, J.J. and Solari, A. (2010),*The sequential rejection principle of familiywise error control*, Annals of Statistics, 38, 3782–3810.

Hansen and Lunde (2006), *Realized variance and market microstructure noise*, Journal of Business & Economic Statistics 24 (2), 127–161.

Hanson, S.G. and Stein, J.C. (2015) *Monetary policy and long-term real rates*, Journal of Financial Economics 115, 429–448.

Henry, T. and Phillips, P.C.B. (2020), *Forecasting economic activity using the yield curve: Quasi-real-time applications for New Zealand, Australia and the US*, Cowles Foundation Discussion Papers. 2574.

Hördahl, P., Remolona, E.M. and Valente, G. (2020) *Expectations and Risk Premia at 8:30*

a.m.: Deciphering the Responses of Bond Yields to Macroeconomic Announcements, Journal of Business and Economic Statistics 38, 27–42.

Hsu, J.C. and Berger, R.L. (1999), *Stepwise confidence intervals without multiplicity adjustment for dose-response and toxicity studies*, Journal of the American Statistical Association 94,468–482.

Jacod, J., Li, Y., Mykland, P.A., Podolskij, M., Vetter, M., 2009. Microstructure noise in the continuous case: the pre-averaging approach. Stochastic Processes and their Applications 119 (7), 2249–2276.

Jacod, J. and Todorov, V. (2009) *Testing for common arrivals of jumps for discretely observed multidimensional processes*. Annals of Statistics 37, 1792–1838.

Jiang, G., Lo, I., and Verdelhan, A. (2011) *Information Shocks, Liquidity Shocks, Jumps, and Price Discovery: Evidence from the U.S. Treasury Market*, Journal of Financial and Quantitative Analysis 46, 527–551.

Koike, Y. (2016) *Estimation of integrated covariances in the simultaneous presence of nonsynchronicity, microstructure noise and jumps*, Econometric Theory 32, 533–611.

Lahaye, J., Laurent, S. and Neely, C.J. (2011) *Jumps, cojumps and macro announcements*, Journal of Applied Econometrics 26 (6), 893–921.

Lee, S. (2012) *Jumps and information flow in financial markets*, Review of Financial Studies 25, 439—479.

Lee, S. and Mykland, P.A. (2008) *Jumps in financial markets: a new nonparametric test and jump dynamics*, Review of Financial Studies 21, 2535–2563.

Lee, S. and Mykland, P.A. (2012) *Jumps in equilibrium prices and market microstructure noise*, Journal of Econometrics 168 (2), 396–406.

Leombroni, M., Vedolinb, A., Venter, G. and Whelan, P. (2021) *Central bank communication and the yield curve*, Journal of Financial Economics 141, 860–880.

Li, J., Todorov, V. and Tauchen, T. (2017) *Jump regression*, Econometrica 85, 173–195.

Li, J., Todorov, V. and Zhang, Q. (2021) *Testing the dimensionality of policy shocks*, working paper.

Marcus, R., Peritz, E. and Gabriel, K.R. (1976), *On closed testing procedures with special reference to ordered analysis of variance*, Biometrika, 63, 655–660.

Pástor, L. and Veronesi, P. (2012) *Uncertainty about government policy and stock prices*, Journal of Finance 67, 1219–1264.

Podolskij, M., Vetter, M., 2009. Estimation of volatility functionals in the simultaneous presence of microstructure noise and jumps. Bernoulli 15 (3), 634–658.

Podolskji, M. and Ziggel, D. (2010), *New tests for jumps in semimartingale models*, Stat. Inference Stoch. Process. 13 (1), 15–41.

Swanson E.T. (2021), *Measuring the effects of federal reserve forward guidance and asset purchases on financial markets*, Journal of Monetary Economics 118, 32–53.

Winkelmann, L., Bibinger, M. and Linzert, T. (2016) *ECB monetary policy surprises: Identification through cojumps in interest rates*, Journal of Applied Econometrics 31 (4), 613–629.

Yang,P.R. (2020) *Using the yield curve to forecast economic growth*, Journal of Forecasting 39, 1057–1080.

SUPPLEMENTARY ONLINE APPENDIX

A Assumptions

In this appendix, we are more precise about the underlying semimartingale model which directly translates from Bibinger et al. (2019). The assumptions impose the maximal degree of generality that still allow the estimation of pre-averaged prices (3) and returns (4) in the context of Proposition 2.1. We consider (1) on some filtered probability space $(\Omega, \mathcal{F}, (\mathcal{F}_t), \mathbb{P})$. The jumps J_t in (1) are split into compensated (small) jumps and finitely many large jumps:

$$J_t = \int_0^t \int_{\mathbb{R}^2} \delta(s,z) \mathbb{1}_{\{|\delta(s,z)|\leq 1\}} (\mu - \nu)(ds,dz) + \int_0^t \int_{\mathbb{R}^2} \delta(s,z) \mathbb{1}_{\{|\delta(s,z)|>1\}} \mu(ds,dz), \qquad (15)$$

with the jump size function δ, defined on $\Omega \times \mathbb{R}_+ \times \mathbb{R}^2$, and the Poisson random measure μ, which is compensated by $\nu(ds,dz) = \lambda(dz) \otimes ds$ with a σ-finite measure λ. The smoothness of the elements of the drift $b_t^{(i)}$ and $\sigma_t^{(i,j)}$, $i,j = a,b$ of spot squared volatility $\Sigma_t = \sigma_t \sigma_t'$ is defined by the following assumption:

Assumption 1 *In* (1)*, for assets* $i,j = a,b$*, the drift* $(b_t^{(i)})_{t\geq 0}$ *is a locally bounded process. The volatilities never vanish,* $\inf_{t\in[0,1]} \sigma_t^{(i,i)} > 0$ *almost surely. For all* $0 \leq t+s \leq 1$*,* $t \geq 0$*, some constants* $C_n, \tilde{C}_n > 0$*, some* $\beta > 1/2$ *and for a sequence of stopping times* T_n *increasing to* ∞*, we have that*

$$\left| \mathbb{E}\big[\sigma^{(i,j)}_{(t+s)\wedge T_n} - \sigma^{(i,j)}_{t\wedge T_n} \,|\mathcal{F}_t \big] \right| \leq C_n \, s^{\beta} \,, \qquad (16)$$

$$\mathbb{E}\Big[\sup_{\mathrm{t}\in[0,s]} |\sigma^{(i,j)}_{(\mathrm{t}+t)\wedge T_n} - \sigma^{(i,j)}_{t\wedge T_n}|^2 \Big] \leq \tilde{C}_n \, s \,. \qquad (17)$$

We impose the following regularity conditions on the (co)jumps

Assumption 2 *Assume for the predictable function δ in (15) that $\sup_{\omega,x} |\delta(t,x)|/\gamma(x)$ is locally bounded with a non-negative deterministic function γ that satisfies*

$$\int_{\mathbb{R}^2} (\gamma^r(x) \wedge 1)\lambda(dx) < \infty\,, \tag{18}$$

with jump activity index r, $0 \leq r < 4/3$.

The index r in (18) measures the (co)jump activity of the bond yields in (1). Smaller values of r make (16) more restrictive. $r = 0$ results in finite-activity jumps and $r = 1$ implies jumps that are summable. The upper bound on r is proved by Bibinger et al. (2019) to make the univariate version of Proposition 2.1 hold.

B Proof

Proposition 2.1

We fill the missing part of the proof of Proposition 3.1 of Bibinger et al. (2019) for the bivariate model. We state here only the crucial extensions of the covariance of the Brownian component and the noise. The higher order n of the drift part allows us to neglect the drifts. Properties of the pre-averaged estimator (drift, Brownian and jump parts) for the individual bonds $i = a, b$, including the mixed normality is shown in Bibinger et al. (2019), and carry over to the bivariate setting. Hence the missing part which proves Proposition 2.1 is the covariance between the Brownian components C_t and noise ϵ of the two assets at some known stopping time τ, respectively.

We rewrite the vector of pre-averaged returns of the observed yields in terms of increments $\Delta\tilde{y}_i = \tilde{y}_i - \tilde{y}_{i-1}$, and study the independent Brownian and noise component

separately.

$$M_n^{-1}\left(\sum_{k=0}^{M_n-1}\tilde{y}_{\tau n+k}-\sum_{k=-M_n}^{-1}\tilde{y}_{\tau n+k}\right)=M_n^{-1}\sum_{k=0}^{M_n-1}(\tilde{y}_{\tau n+k}-\tilde{y}_{\tau n+k-M_n})$$
$$=M_n^{-1}\left(\sum_{k=1}^{M_n-1}\Delta\tilde{y}_{\tau n+k}(M_n-k)+\sum_{k=0}^{M_n-1}\Delta\tilde{y}_{\tau n-k}(M_n-k)\right) \tag{19}$$

The strategy of the proof in Bibinger et al. (2019) is then to exploit the above equation with respect to the individual signal parts of the process $y_t^{(i)}$, $i=a,b$ in (2) and (1). For the covariance of the increments of the Brownian components this gives:

$$\begin{aligned}\mathrm{Cov}\Bigg[&\sum_{k=1}^{M_n-1}\Delta C^{(a)}_{(\tau n+k)/n}\frac{M_n-k}{M_n}+\sum_{k=0}^{M_n-1}\Delta C^{(a)}_{(\tau n-k)/n}\frac{M_n-k}{M_n},\\&\sum_{k=1}^{M_n-1}\Delta C^{(b)}_{(\tau n+k)/n}\frac{M_n-k}{M_n}+\sum_{k=0}^{M_n-1}\Delta C^{(b)}_{(\tau n-k)/n}\frac{M_n-k}{M_n}\Bigg]\\&=\sum_{k=1}^{M_n-1}\mathrm{E}\left[\Delta C^{(a)}_{(\tau n+k)/n}\Delta C^{(b)}_{(\tau n+k)/n}\right]\left(1-\frac{k}{M_n}\right)^2\\&\quad+\sum_{k=0}^{M_n-1}\mathrm{E}\left[\Delta C^{(a)}_{(\tau n-k)/n}\Delta C^{(b)}_{(\tau n-k)/n}\right]\left(1-\frac{k}{M_n}\right)^2,\end{aligned}$$

with uncorrelated increments on disjoint intervals in case of stochastic volatility. Itô isometry,

$$\mathrm{E}\left[\int_0^t\sigma_s^{(a,a)}dW_s^{(a)}\int_0^t\sigma_s^{(b,b)}dW_s^{(b)}\right]=\int_0^t\mathrm{E}[\sigma_s^{(a,a)}\sigma_s^{(b,b)}]\rho_s^{(a,b)}ds,$$

and the smoothness of the volatility and correlation imply that

$$\begin{aligned}\mathrm{E}\left[\Delta C^{(a)}_{(\tau n+k)/n}\Delta C^{(b)}_{(\tau n+k)/n}|\mathcal{F}_\tau\right]&=\mathrm{E}\left[\int_{(\tau n+k-1)/n}^{(\tau n+k)/n}\sigma_s^{(a,b)}ds|\mathcal{F}_\tau\right]+\mathcal{O}_P(n^{-2})\\&=\frac{\rho_\tau^{(a,b)}\sigma_\tau^{(a,a)}\sigma_\tau^{(b,b)}}{n}+\mathcal{O}_P\left(\sqrt{\frac{M_n}{n}}n^{-1}\right)\end{aligned}$$

for $k = 1, ..., M_n - 1$. Similarly, we obtain to the left of τ

$$\begin{aligned} \mathrm{E}\left[\Delta C^{(a)}_{(\tau n-k)/n}\Delta C^{(b)}_{(\tau n-k)/n}|\mathcal{F}_\tau\right] &= \mathrm{E}\left[\int_{(\tau n-k-1)/n)}^{(\tau n-k)/n} \sigma_s^{(a,b)} ds|\mathcal{F}_\tau\right] + \mathcal{O}_P(n^{-2}) \\ &= \frac{\rho^{(a,b)}_{\tau-}\sigma^{(a,a)}_{\tau-}\sigma^{(b,b)}_{\tau-}}{n} + \mathcal{O}_P\left(\sqrt{\frac{M_n}{n}}n^{-1}\right). \end{aligned}$$

The increments in *iid* noise contribute

$$\mathrm{E}\left[\Delta\epsilon^{(a)}_{\tau n-k}\Delta\epsilon^{(b)}_{\tau n-k}|\mathcal{F}_\tau\right] = \mathrm{E}\left[(\epsilon^{(a)}_{\tau n-k} - \epsilon^{(a)}_{\tau n-k-1})(\epsilon^{(b)}_{\tau n-k} - \epsilon^{(b)}_{\tau n-k-1})\right] = 2\eta^{(a,b)}.$$

Finally, in conjunction with the identities

$$\sum_{k=1}^{M_n-1}\left(1-\frac{k}{M_n}\right)^2 = \frac{1}{3}M_n - \frac{1}{2} + \frac{1}{6}M_n^{-1}, \quad \text{and} \quad \sum_{k=0}^{M_n-1}\left(1-\frac{k}{M_n}\right)^2 = \frac{1}{3}M_n + \frac{1}{2} + \frac{1}{6}M_n^{-1},$$

we obtain the asymptotic covariance of event returns of asset a and b:

$$\sqrt{M_n}\mathrm{E}\left[\Delta\hat{y}^{(a)}_{\tau n}\Delta\hat{y}^{(b)}_{\tau n}\right] \to \left(\frac{\rho^{(a,b)}_{\tau}\sigma^{(a,a)}_{\tau}\sigma^{(b,b)}_{\tau}}{3} + \frac{\rho^{(a,b)}_{\tau-}\sigma^{(a,a)}_{\tau-}\sigma^{(b,b)}_{\tau-}}{3}\right)c^2 + 2\eta^{(a,b)}. \tag{20}$$

■

C Data on government bonds

Tables A.1 provides information on the U.S. Treasury bonds used in the empirical analyses. We use maturities that are closest to 2, 10 and 20 years at the time of each news release as proxies to extract data on the bond yields.

Table A.1: The list of U.S. Treasury bonds used in the empirical analyses.

Treasury Inflation-Protected Securities					
CUSIP	Coupon	Maturity	CUSIP	Coupon	Maturity
912828GD6	2.375	1/15/2017	912828SA9	0.125	1/15/2022
912828SQ4	0.125	4/15/2017	912810FR4	2.375	1/15/2025
912828GX2	2.625	7/15/2017	912828H45	0.250	1/15/2025
912828HN3	1.625	1/15/2018	912828XL9	0.375	7/15/2025
912828UX6	0.125	4/15/2018	912828N71	0.625	1/15/2026
912828JE1	1.375	7/15/2018	912828S50	0.125	7/15/2026
912828JX9	2.125	1/15/2019	912828V49	0.375	1/15/2027
912828C99	0.125	4/15/2019	9128282L3	0.375	7/15/2027
912828LA6	1.875	7/15/2019	9128283R9	0.500	1/15/2028
912828MF4	1.375	1/15/2020	912810FD5	3.625	4/15/2028
912828K33	1.375	4/15/2020	912828Y38	0.750	7/15/2028
912828NM8	1.250	7/15/2020	9128285W6	0.875	1/15/2029
912828PP9	1.125	1/15/2021	912810FH6	3.875	4/15/2029
912828Q60	0.125	4/15/2021	9128287D6	0.250	7/15/2029
912828QV5	0.625	7/15/2021	912828Z37	0.125	1/15/2030
Treasury Bonds					
CUSIP	Coupon	Maturity	CUSIP	Coupon	Maturity
912810DX3	7.500	11/15/2016	912810EY0	6.500	11/15/2026
912810DY1	8.750	5/15/2017	912810EZ7	6.625	2/15/2027
912810DZ8	8.875	8/15/2017	912810FA1	6.375	8/15/2027
912810EA2	9.125	5/15/2018	912810FB9	6.125	11/15/2027
912810EB0	9.000	11/15/2018	912810FE3	5.500	8/15/2028
912810EC8	8.875	2/15/2019	912810FF0	5.250	11/15/2028
912810ED6	8.125	8/15/2019	912810FG8	5.250	2/15/2029
912810EE4	8.500	2/15/2020	912810FJ2	6.125	8/15/2029
912810EF1	8.750	5/15/2020	912810FP8	5.375	2/15/2031
912810EG9	8.750	8/15/2020	912810FT0	4.500	2/15/2036
912810EH7	7.875	2/15/2021	912810PT9	4.750	2/15/2037
912810EJ3	8.125	5/15/2021	912810PU6	5.000	5/15/2037
912810EK0	8.125	8/15/2021	912810PW2	4.375	2/15/2038
912810EL8	8.000	11/15/2021	912810PX0	4.500	5/15/2038
912810ES3	7.500	11/15/2024	912810QA9	3.500	2/15/2039
912810ET1	7.625	2/15/2025	912810QB7	4.250	5/15/2039
912810EV6	6.875	8/15/2025	912810QC5	4.500	8/15/2039
912810EW4	6.000	2/15/2026	912810QD3	4.375	11/15/2039
912810EX2	6.750	8/15/2026	912810QE1	4.625	2/15/2040

Diskussionsbeiträge - Fachbereich Wirtschaftswissenschaft - Freie Universität Berlin
Discussion Paper - School of Business & Economics - Freie Universität Berlin

2021 erschienen:

2021/1 HÜGLE, Dominik: Higher education funding in Germany: a distributional lifetime perspective
Economics

2021/2 ISHAK, Phoebe W.: Murder Nature: Weather and Violent Crime in Brazil
Economics

2021/3 STEINER, Viktor und Junyi ZHU: A Joint Top Income and Wealth Distribution
Economics

2021/4 PIPER, Alan: An economic analysis of the empty nest syndrome: what the leaving child does matters
Economics

2021/5 DEISNER, Jana; Johanna MAI und Carolin AUSCHRA: The social (de-) construction of the Corona-pandemic as being a serious threat to society: insights from a discource analysis of German tweets until contacts were banned in March 2020
Management

2021/6 DIECKELMANN, Daniel: Market Sentiment, Financial Fragility, and Economic Activity: the Role of Corporate Securities Issuance
Economics

2021/7 SCHREIBER, Sven und Vanessa SCHMIDT: Missing growth measurement in Germany
Economics

2021/8 HÜGLE, Dominik: The decision to enrol in higher education
Economics

2021/9 ZUCKER MARQUES, Marina: Financial statecraft and transaction costs: the case of renminbi internationalization
Economics

2021/10 EVERS, Andrea und Eva K. MATTHAEI: Steuerplanung unter Unsicherheit: eine Befragungsstudie zum Brexit
FACTS

2021/11 BESTER, Helmut: Fairness and Competition in a Bilateral Matching Market
Economics

2021/12 COLEMAN, Winnie und Dieter NAUTZ: Inflation Expectations, Inflation Target Credibility and the COVID-19 Pandemic: New Evidence from Germany
Economics

2021/13 AMBROSIUS, Christian; Raymundo M. CAMPOS-VÁZQUEZ und Gerardo ESQUIVEL: What Drives Remittances During a Global Shock?: Evidence from the COVID-19 Pandemie in Mexico
Economics

2021/14 REISS, Markus und Lars WINKELMANN: Inference on the Maximal Rank of Time-Varying Covariance Matrices Using High-Frequency Data
Economics